Journal of Engineering and Sustainable Development
http://jeasd.uomustansiriyah.edu.iq/index.php
https://doi.org/10.31272/jeasd.26.4.8

Vol. 26, No. 04, July 2022
ISSN 2520-0917

FINITE ELEMENT ANALYSIS OF A SINGLE-PHASE INDUCTION MOTOR WITH NON-UNIFORM STATOR SLOTS BASED ON MAGNET SOFTWARE AND AUTOCAD

Marwa A. Dawood **Amer M. Ali**

Electrical Engineering Department, College of Engineering, Mustansiriyah University, Baghdad, Iraq

Received 6/11/2021 ***Accepted in revised form 18/1/2022*** ***Published 1/7/2022***

Abstract: The current study uses the finite element technique to investigate a single-phase induction motor with non-uniform stator slots. A 0.5 hp, four poles, 36 stator slots, and 48 rotor slots have non-uniform stator slots was analyzed based on magnet Finite Element Method software with using AutoCAD in modeling stator due to its unsymmetrical slots, The suggested study attempts to evaluate all motor design modifications. The values of currents and torque received from the FEM analysis for test motor were compared with motor nameplate data with a good agreement.

Keywords: *Single-phase induction motor, non-uniform stator slots, finite element analysis, Magnet.*

1. Introduction

SPIMS are broadly used in a variety of applications in both the home and the workplace. As a result, compliance with noise and vibration standards is necessary with any device. From the stand point of the motor designer, new as well as precise approaches for motor design are required, as well as compliance with noise and vibration Standards. Finite Element Method (FEM) is adopted for this motor because it provide a high results accuracy by accounting for the skin effect in rotor bars, non-linearity of core electrical steel, and motor parameter changes as a function of load [1]. The analysis of SPIMS must be taken into consideration the rotating field theory, which states there are two types of rotating magnetic waveforms in the machine: one is direct and the other is inverse; the phase angle is achieving by connecting an indefinitely large capacitor in series with the auxiliary winding.

When it comes to mathematical modeling, single-phase motors look simple, but their elliptical rotating electromagnetic field complicates things. This can be worked around using the revolving filed polygon technique, which is widely used in the industry to accurately predict motor operating characteristics [2],[3].

Many researches were presented for studying the single phase capacitor motor by utilization the FEM to evaluate its performance in order to enhance its efficiency, starting torque, and

**Corresponding Author*: madsf1990@gmail.com

calculate its parameters. Hori has developed a unique starting performance analysis.by Using a multi slice model, 2-D time-stepping FEA in order to correctly forecast the beginning performance of the prototype motor [4].Krikor investigates the single-phase capacitor motor's starting performance as well as the influence of the motor capacitor on the beginning performance. analytical technique is builds on a 2-D FEM using ANSYS software [5]. Karpe uses the SPIM design optimization approach to maximize efficiency while keeping material and tooling costs to a minimum. A 0.5 horsepower, two-pole motor was used as a test case in this study. The double revolving theory is used to provide design ideas for capacitor start and run motor optimization. Finite Element Study is used to validate the optimized design [6]. When designing single-phase induction motors, Wang uses an equivalent circuit approach and a voltage source complicated finite-element model to achieve a balance between accuracy and efficiency [7]. The present paper aims to use the finite element analysis on a 1/2 hp single-phase capacitor motor have non-uniform stator slots based on Magnet software and AutoCAD to model a non-uniform stator slots.

2. Mathematical Background

The designing of the electrical machines was reinforced through numerical analysis, which was frequently builds on the finite element method and Maxwell's equations, which are solved through partition motor cross section area into several elements, every one of which contains the magnetic vector potential A and, as a result, the magnetic flux density distribution B. The analytical approach to calculating magnetic flux density in the multiple areas of the motor construction is frequently insufficiently accurate because it depends on approximations. As a result, the exact motor geometry, as well as the properties of all materials, are entered into FEM software, allowing for accurate computation of magnetic flux density distribution throughout the whole cross section of the motor. An adequate conclusion on core saturation in the motor model can be obtained by appropriately interpreting the acquired results. Furthermore, the numerical analysis may be utilized to compute multiple motor parameters, such as starting torque of the motor.

The domain of the examined object is discretized using FEM, which results in a group of matrix differential equations. The temporal decomposition method is used to solve them (TDM). The domain is divided along time axis, as well as rather than solving each time step individually, all time steps are solved concurrently .The Maxwell's equations are listed below [8] :

$$\nabla \times E = \frac{-\partial B}{\partial t} \tag{1}$$

$$\nabla \times H = J + \frac{\partial D}{\partial t} \tag{2}$$

$$\nabla \cdot D = \rho \tag{3}$$

$$\nabla \cdot B = 0 \tag{4}$$

The intensity of the electric field is also linked to the electric current density (J) as follow:

$$J = \sigma E \tag{5}$$

Maxwell's equations define the electromagnetic prodigies in a static and moving reference frame as-

$$B^* = B \tag{6}$$

$$E^* = E + v \times B \tag{7}$$

$$H^* = H \tag{8}$$

$$J^* = J \tag{9}$$

A moving reference frame is shown by quantities on the right hand side, whereas the electric field vector E only has a single quantity changed. The magnetic field density divergence may be calculated using the following formula:

$$\nabla \cdot B^{*} = 0 \qquad (10)$$

The magnetic vector potential may be expressed as:

$$\nabla \cdot (v \, \nabla A) = -J \qquad (11)$$

$$J = \sigma E^{*} = \sigma (E + v \times B) \qquad (12)$$

3. Test Motor Modeling

The first step in defining the FEM model for motor is the entry of the exact motor geometry and properties of the motor materials. The auxiliary and the main winding, made of copper wire, are placed in the auxiliary and the main stator slots, while the rotor winding is of squirrel cage type with the rotor cage made of aluminum. The core is made from silicon steel according to its BH curve. A 25µF capacitor is permanently connected in the auxiliary winding during the motor start-up, and during continuous operation of the motor.

A Magnet software model is made from a geometric model. The finite element mesh of the model is shown in figures (1) & (2),

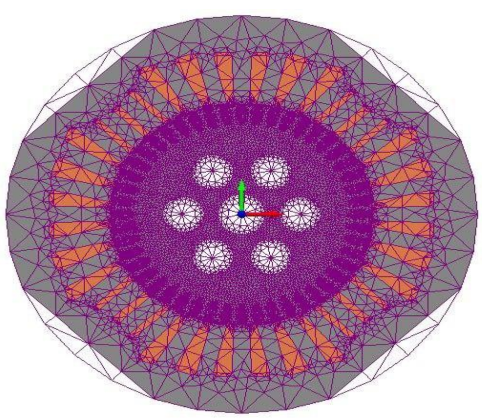

Figure 1. Test motor model meshing by magnet

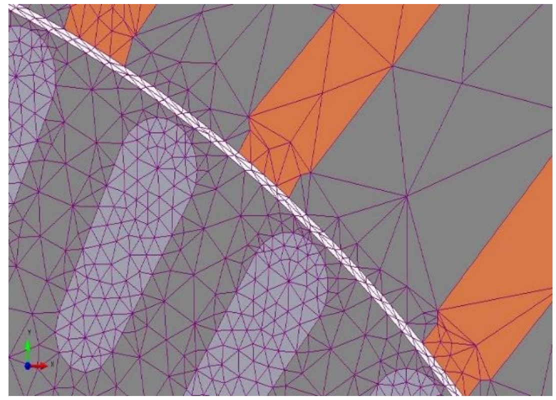

Figure 2. Enlarged view of air gap meshing

The two stator windings (main and auxiliary) are defined by stranded conductors and the resistance for each phase is specified; and, a voltage source component is defined by the standard sinusoidal signal formulation. For the front and rear sections of the stator windings, which cannot be represented using two-dimensional finite elements, two resistances and inductances are employed, which must be computed using characteristics like number of stator slots ,the turns per slot, and poles per phase, and the number of the parallel coils [9] . Figure 3 indicate the electrical circuit connection of test motor using Magnet software.

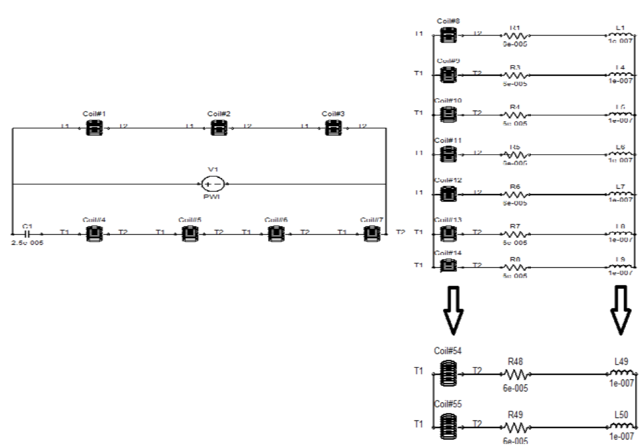

Figure 3. The electric circuit of the test motor by magnet

The stator model has been drawn by AutoCAD software because of non-uniform stator slots. After that the model was import to the magnet software and divided it into 8 slices to include the rotor bars skewing in calculations, and connected these slices electrically in series as shown in figure (4). The core stack length equal to 35mm ,the thickness of each slice equal to 4.37mm,the total skewing angle equal to 12 degree , the angle of each slice equal to 1.7 degree. The summation of solution result of each slice give the total motor solution results.

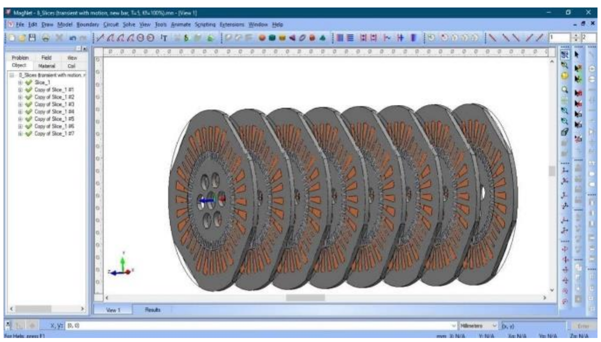

Figure 4. Divided of model in to 8 slices using Magnet software

Figures (5)&(6) show the schematics of stator and rotor lamination of SPIM which manufactured in state company of electrical and electronic Industries in Baghdad-Waziriya

Table 1. Data of test motor (SPIM)

Number of stator slots	36
Outer diameter of stator	160.25 mm
Inner diameter of stator	88.90 mm
Iron stack length	35 mm
Number of rotor slots	48
Outer diameter of rotor	88.34 mm
Inner diameter of rotor	16.147 mm
Air-gap length	0.28mm
Rated power output	0.5 hp
Rated voltage	220 V
Number of poles	4
Capacitor	25μF

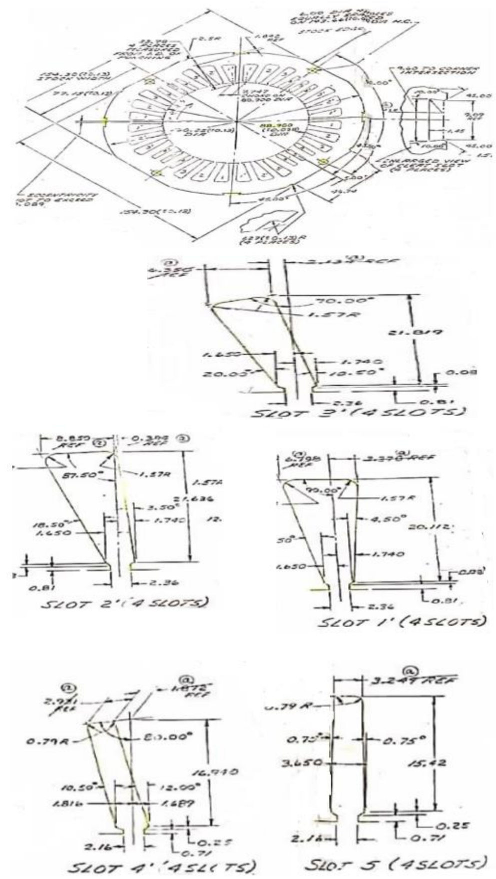

Figure 5. Stator Lamination of SPIM

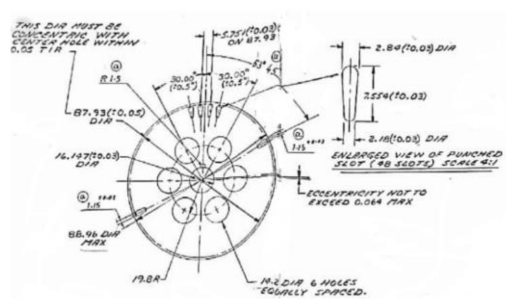

Figure 6. Rotor Lamination of SPIM

4. Results and Discussion

To check the validity of the FEM test motor model we solve it under full load conditions. Figures (7) & (8) illustrate the distribution of

Table 2. Comparison between FEM results and test motor name plate data

	FEM results	name plate Data	Error
Rated current	2.812 A	2.8A	0.355%
Rated torque	2.582	2.5 N.M	3.175%

magnetic flux lines and magnetic flux density in multiple portions of motor model. We observed from these two figures the logical distribution of the magnetic flux and levels of magnetic saturation in motor, which provide a good indicator to validity of the FEM test motor model for further investigation on it.

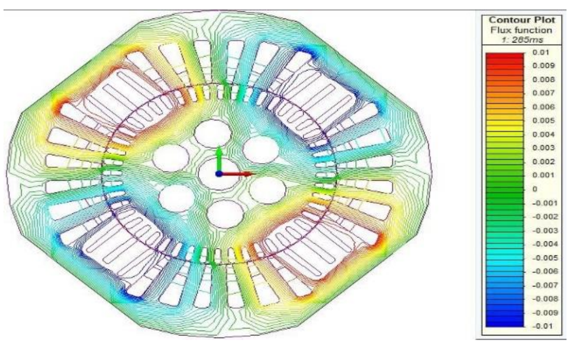

Figure 7. Magnetic flux lines

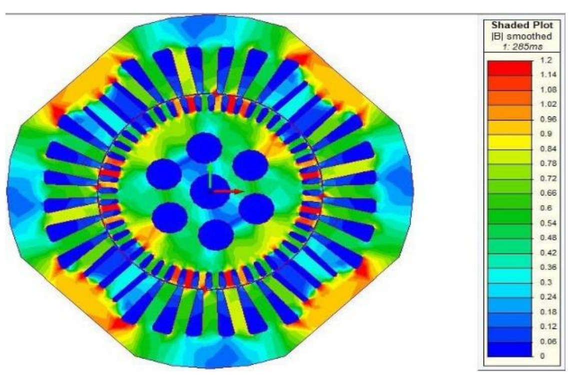

Figure 8. Magnetic flux density

Figure (9) shows the relation between the auxiliary current and time it can be clearly that the root mean square (rms) of auxiliary current is 2.292 A.

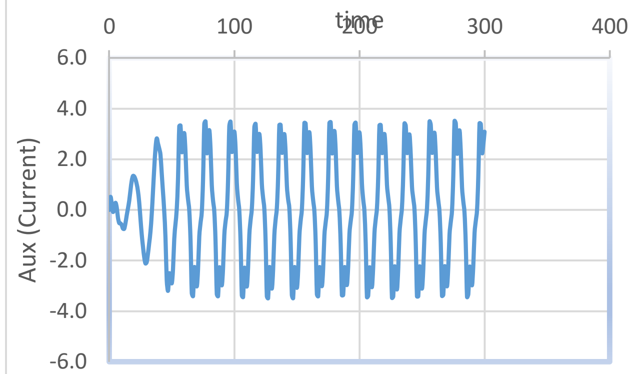

Figure 9 .Auxiliary winding current waveform

Figure 10. shows the relation between the main current and time. The rms of main current is 4.782A

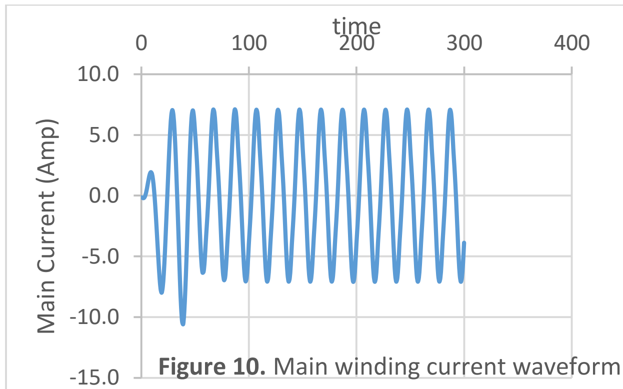

Figure 10. Main winding current waveform

Figure 11. shows the relation between the rated current and time. The rms of rated current is 2.812 A.

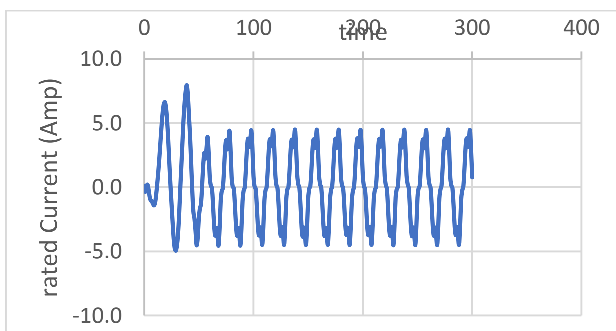

Figure 11. rated current waveform

Figure 12. shows the relation between the torque and time. the rated torque is 2.5821 N.m.

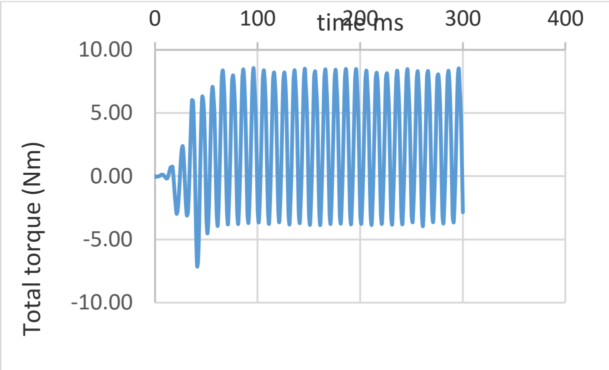

Figure 12. rated torque waveform

5. Conclusion

A single-phase capacitor motor with non-uniform stator slots has been successfully modeled and analyzed by Magnet software with assist of AutoCAD. The values of currents and torque received from the finite element analysis for test motor were compared to with their values in motor name plate data with a good agreement.

Acknowledgements

Thanks for Dr. Ahmed Muhammad, Electrical Engineering Department, University of Technology, for his support in using Magnet software. In addition, thanks extended to Electrical Engineering Department, College of Engineering, Mustansiriyah University.

Conflict of interest

The authors demonstrate that the publication of this article produce no conflict of interest.

Abbreviations

E	Electric field intensity
D	Electric flux density
H	Magnetic field intensity
J	Electric current density
B	Magnetic field density
ρ	Electric charge density
A	Magnetic vector potential
V	Moving velocity

6. References

1. A. Negoita, G. Scutaru, I. Peter, R. M. Ionescu, O. Plesa, and C. Nistor, “Numerical modeling and experimental analysis of the magnetic noise of the single-phase, inverter-fed permanent split-capacitor motor,” Proc. Int. Conf. Optim. Electr. Electron. Equipment, OPTIM, pp. 600–605, 2012, doi: 10.1109/OPTIM.2012.6231892.
2. V. Sarac and N. TRAJCHEVSKI, “Impact of capacitor on operating characteristics of single-phase motor,” in 2019 16th Conference on Electrical Machines, Drives and Power Systems (ELMA), 2019, pp. 1–5.
3. A. Leicht and K. Makowski, “Analysis of a single-phase capacitor induction motor operating at two power line frequencies,” Arch. Electr. Eng., vol. 61, no. 2, pp. 251–266, 2012.
4. M. Hori, K. Kurihara, and T. Kubota, “Starting performance analysis for a single-phase capacitor-run permanent magnet motor with skewed rotor slots,” in 2008 18th International Conference on Electrical Machines, 2008, pp. 1–6.
5. S. K. Krikor, Y. M. Dhari, and K. Y. Maha, “Starting performance analysis of single-phase capacitor motor using finite element method,” Eng. Tech., vol. 26, no. 8, 2008.
6. M. Karpe, S. Ghosh, N. Shindhe, R. Birajdar, and D. Bhave, “Optimization of Single-Phase Induction Motor,” in 2019 IEEE Conference on Energy Conversion (CENCON), 2019, pp. 115–120.
7. X. Wang, C. Zhu, R. Zhang, R. Tang, and H. Song-Yop, “Performance analysis of single-phase induction motor based on voltage source complex finite-element

analysis," IEEE Trans. Magn., vol. 42, no. 4, pp. 587–590, 2006.

8. O. J. Tola, E. A. Umoh, E. A. Yahaya, C. Idoko, and A. Imoru, "Electromagnetic Field analysis of a Single-phase Induction Motor based on Finite Element Method."
9. I. Boldea and S. A. Nasar, Electric drives. CRC press, 2016.